International Journal of Bifurcation and Chaos, Vol. 23, No. 5 (2013) 1330014 (17 pages)

DOI: 10.1142/S0218127413300140

CHAOS ENTANGLEMENT: A NEW APPROACH TO GENERATE CHAOS

HONGTAO ZHANG* and XINZHI LIU†
Department of Applied Mathematics, University of Waterloo,
200 University Avenue West, Waterloo,
Ontario N2L 3G1, Canada
**h15zhang@gmail.com*
†*xzliu@math.uwaterloo.ca*

XUEMIN SHEN
Department of Electrical and Computer Engineering,
University of Waterloo, 200 University Avenue West,
Waterloo, Ontario N2L 3G1, Canada
xshen@bbcr.uwaterloo.ca

JUN LIU
Department of Automatic Control and Systems Engineering,
University of Sheffield, Mappin Street,
Sheffield, Yorkshire S1 3JD, UK
j.liu@sheffield.ac.uk

Received May 4, 2012; Revised September 15, 2012

A new approach to generate chaotic phenomenon, called chaos entanglement, is proposed in this paper. The basic principle is to entangle two or multiple stable linear subsystems by entanglement functions to form an artificial chaotic system such that each of them evolves in a chaotic manner. Firstly, a new attractor, entangling a two-dimensional linear subsystem and a one-dimensional one by sine function, is presented as an example. Dynamical analysis shows that both entangled subsystems are bounded and all equilibra are unstable saddle points when chaos entanglement is achieved. Also, numerical computation shows that this system has one positive Lyapunov exponent, which implies chaos. Furthermore, two conditions are given to achieve chaos entanglement. Along this way, by different linear subsystems and different entanglement functions, a variety of novel chaotic attractors have been created and abundant complex dynamics are exhibited. Our discovery indicates that it is not difficult any more to construct new artificial chaotic systems/networks for engineering applications such as chaos-based secure communication. Finally, a possible circuit is given to realize these new chaotic attractors.

Keywords: Chaotic attractor; chaos entanglement; Lyapunov exponent; bifurcation; chaos circuit.

1. Introduction

Chaos phenomenon, characterized by "butterfly effect", i.e. the dynamical behavior of a nonlinear system is highly sensitive to initial conditions, rendering long-term prediction impossible in general, has been found in many fields such as physics, biology, economics, engineering, etc. For instance, in [Lorenz, 1963] the Lorenz system was presented, a mathematical model for weather prediction, which shows that even detailed atmospheric model cannot make long-term weather predictions. Weather is usually predictable only about a week ahead

[Watts, 2007]. Matsumoto [1984] introduced Chua's circuit, the first chaotic electronic circuit, which makes itself a ubiquitous real-world example of a chaotic system. With chaos theory actively developing, scientists also transferred their research focus from controlling and eliminating chaos in the early stage to applying chaos in practice recently. Specifically, since chaos synchronization was presented by [Pecora & Carroll, 1990], chaotic systems became useful tools in engineering applications such as the chaotic carrier in secure communication. Accordingly, the requirement for creating new chaotic systems is dramatically increasing. Currently, designing and constructing new artificial chaotic systems has become an active issue.

By and large, extending and improving the existing chaotic systems, such as Lorenz system, Chua's circuit, Mackey–Glass system [Mackey & Glass, 1977], etc., to more complex dynamics is an important way to generate new chaotic attractors. Deriving from Lorenz system, Chen and Ueta [1999] presented the Chen system, which is not topologically equivalent to the Lorenz system. Subsequently, Lü and Chen [2002] found the Lü system, different from the two formers in the sense of Vaněček–Čelikovský classification [Vaněček & Čelikovský, 1996]. A generalized Lorenz canonical form of chaotic systems was established [Čelikovský & Chen, 2002]. Multiscroll chaotic and hyperchaotic attractors generated from Chen system was presented in [Liu *et al.*, 2012]. Deriving from Chua's circuit, a lot of multiscroll chaotic attractors and hyperchaotic attractors were reported. Firstly, Suykens and Vandewalle [1993] introduced n-double scroll attractors. Yalçin *et al.* [2002] presented multiscroll grid attractors using a step function approach, and furthermore [Yalçin, 2007] presented multiscroll and hypercube attractors from a general jerk circuit using Josephson junctions. Lü *et al.* [2004b] generated 3-D multiscroll chaotic attractors by a hysteresis series switching method. Yu *et al.* [2007] designed multifolded torus chaotic attractors. A nonautonomous technique to generate multiscroll attractors and hyperchaos has been introduced in [Elwakil & Ozoguz, 2006; Li *et al.*, 2005]. Utilizing switching technology, some new chaotic attractors were found [Lü *et al.*, 2004b; Lü & Chen, 2006; Lü *et al.*, 2004a; Liu *et al.*, 2006]. In addition, fractional differential systems were developed to generate chaos [Hartley *et al.*, 1995; Ahmad & Sprott, 2003; Li & Chen, 2004]. And some circuit implementation have been designed to realize chaos [Yalçin, 2007; Lü *et al.*, 2004b; Chua *et al.*, 1993; Tang *et al.*, 2001; Elwakil & Kennedy, 2001]. Deriving from Mackey–Glass system, a physiological model that possesses chaotic behavior, several modified chaotic systems were reported [Lu & He, 1996; Namajunas *et al.*, 1995; Tamasevicius *et al.*, 2006; Wang & Yang, 2006], in which the authors used a piecewise nonlinearity to replace the original nonlinearity of the Mackey–Glass system. Most recently, Yalçin and Özoguz [2007] presented n-scroll chaotic attractors from a first-order time-delay differential equation. Sprott [2007] found the simplest delay differential equation which can generate a multiscroll chaotic attractor. Zhang *et al.* [2012] created a family of novel chaotic and hyperchaotic attractors from delay differential equation.

It is well known that the Poincaré–Bendixson theorem implies that an autonomous continuous system to generate chaos requires at least three state variables with at least one nonlinearity. It is impossible to generate chaos only by linear systems. However, in reality, linear systems exist far and wide while chaotic systems seem to only exist in rare and specific circumstances. Does there exist a bridge to connect linear systems and chaotic systems such that chaos phenomenon can be generated and observed as generally as what linear systems do? To answer this question, in this paper, we present a new approach, called chaos entanglement, to generate chaos by entangling two or multiple stable linear subsystems. One can entangle three identical one-dimensional stable linear subsystems to generate chaos, or entangle two stable linear subsystems with different system parameters and different dimensions, or even entangle a large number of stable linear subsystems to form an artificial chaotic network. Also, by different entanglement functions such as sine function, piecewise linear function, piecewise sign function, etc., the chaotic attractors generated are totally different. Therefore, it provides an easier way to design and construct new chaotic attractors by chaos entanglement. Chaos entanglement can be utilized as a guideline to effectively create artificial chaotic systems/networks in practice.

The remainder of this paper is organized as follows. In Sec. 2, we construct a new chaotic attractor, entangling a two-dimensional stable linear subsystem and a one-dimensional one by sine function. Chaotic dynamics and boundedness are analyzed in

detail. In Sec. 3, the basic principle of chaos entanglement is introduced. By employing different subsystems and different entanglement functions, we generate a variety of novel chaotic attractors. In Sec. 4, a possible electronic circuit is proposed to realize these new attractors. Finally, conclusions are given in Sec. 5.

2. New Chaotic Attractor

***Chaos entanglement*:** if two or more linear subsystems can behave in chaotic manner when they are entangled by some nonlinear functions, we call it is chaos entanglement. These nonlinear functions are called entanglement functions.

Consider two linear subsystems. One is two-dimensional and the other is one-dimensional,

$$\begin{bmatrix}\dot{x}_1(t)\\ \dot{x}_2(t)\end{bmatrix} = \begin{bmatrix} a_1 & a_2\\ -a_2 & a_1\end{bmatrix}\begin{bmatrix}x_1(t)\\ x_2(t)\end{bmatrix} \tag{1}$$

and

$$\dot{x}_3(t) = a_3 x_3(t), \tag{2}$$

where $x_i(t)$ $(i = 1, 2, 3)$ is the state variable. When $a_1 < 0$ and $a_3 < 0$, both subsystems are stable. We entangle these two subsystems in the following way:

$$\begin{cases}\dot{x}_1(t) = a_1 x_1(t) + a_2 x_2(t)\\ \dot{x}_2(t) = -a_2 x_1(t) + a_1 x_2(t) + b_1 \sin(x_3(t))\\ \dot{x}_3(t) = a_3 x_3(t) + b_2 \sin(x_1(t))\end{cases}$$

where b_i $(i = 1, 2)$ is the entanglement coefficient and $\sin(x_i(t))$ $(i = 1, 3)$ is the entanglement function. It can be rewritten in a compact form:

$$\dot{X} = AX + BF, \tag{3}$$

where

$$X = \begin{bmatrix}x_1(t)\\ x_2(t)\\ x_3(t)\end{bmatrix}, \quad A = \begin{bmatrix} a_1 & a_2 & 0\\ -a_2 & a_1 & 0\\ 0 & 0 & a_3\end{bmatrix},$$

$$B = \begin{bmatrix}0 & 0 & 0\\ 0 & b_1 & 0\\ 0 & 0 & b_2\end{bmatrix}, \quad \text{and} \quad F = \begin{bmatrix}0\\ \sin(x_3(t))\\ \sin(x_1(t))\end{bmatrix}.$$

For $a_1 = -1$, $a_2 = 1$, $a_3 = -1$, $b_1 = 36$, and $b_2 = 18$, system (3) is chaotic. Figure 1 shows the portrait of its two very close trajectories. The blue curve $(x_1(t), x_2(t), x_3(t))$ starts from $(1, -1, -2)$

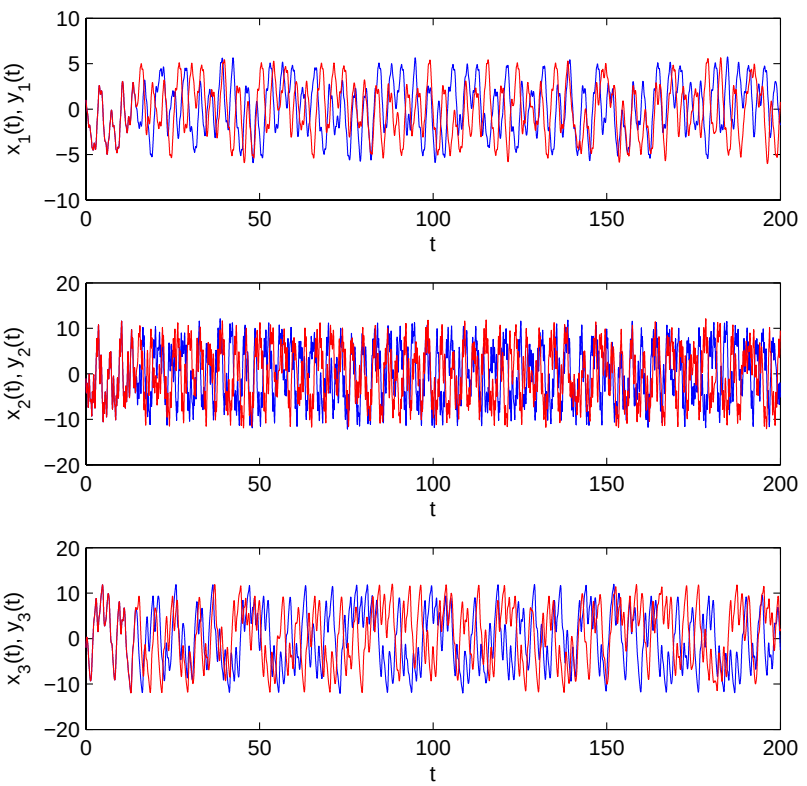

Fig. 1. The trajectory portraits of $(x_1(t), x_2(t), x_3(t))$ and $(y_1(t), y_2(t), y_3(t))$ starting from $(1, -1, -2)$ and $(1, -1, -1.99999)$, respectively, with $a_1 = -1$, $a_2 = 1$, $a_3 = -1$, $b_1 = 36$, and $b_2 = 18$.

and the red curve $(y_1(t), y_2(t), y_3(t))$ starts from $(1, -1, -1.99999)$. The difference at the initial condition, 10^{-5}, is very tiny. It can be observed that after a short time these two trajectories become totally different. This implies that it is impossible that one wants to predict $(x_1(t), x_2(t), x_3(t))$ by $(y_1(t), y_2(t), y_3(t))$, in general. This phenomenon is called "butterfly effect", which is the characteristics of chaotic systems. Figure 2 shows the evolution of the corresponding errors. After $t = 15$ sec, the errors become out of order. Figure 3 shows the phase portraits of system (3).

2.1. *Equilibria*

To analyze the dynamics of system (3), a good start is to find out its equilibria and to study the stability of each equilibrium point. Usually, the equilibria are related to system parameters, which can be calculated by solving the following equation:

$$AX + BF = 0$$

i.e.

$$\begin{cases} a_1 x_1(t) + a_2 x_2(t) = 0 \\ -a_2 x_1(t) + a_1 x_2(t) + b_1 \sin(x_3(t)) = 0 \\ a_3 x_3(t) + b_2 \sin(x_1(t)) = 0. \end{cases} \quad (4)$$

At each equilibrium point $X^* = (x_1^*, x_2^*, x_3^*)^T$, the linearization system of system (3) is given by

$$\dot{X} = JX, \quad (5)$$

where

$$J = \begin{bmatrix} a_1 & a_2 & 0 \\ -a_2 & a_1 & b_1 \cos(x_3^*) \\ b_2 \cos(x_1^*) & 0 & a_3 \end{bmatrix}.$$

The corresponding characteristic equation is

$$\lambda^3 - (2a_1 + a_3)\lambda^2 + (a_1^2 + a_2^2 + 2a_1 a_3)\lambda = (a_1^2 + a_2^2)a_3 + a_2 b_1 b_2 \cos(x_1^*) \cos(x_3^*).$$

Throughout this paper, for simplification, we only consider $a_1 = -a$, $a_2 = a$, $a_3 = -a$, $b_1 = 2b$ and $b_2 = b$ where $a > 0$ and $b > 0$. Then, system (3) turns into a two-parameter system with a and b.

Equation (4) is a transcendental equation set. Usually, it is not easy to find out its accurate solutions. Here, we calculate its numerical approximate solutions by finding the point at which the intersections occur, based on Matlab software. When $a = 1$ and $b = 18$, system (3) has 127 equilibria (shown in Fig. 4).

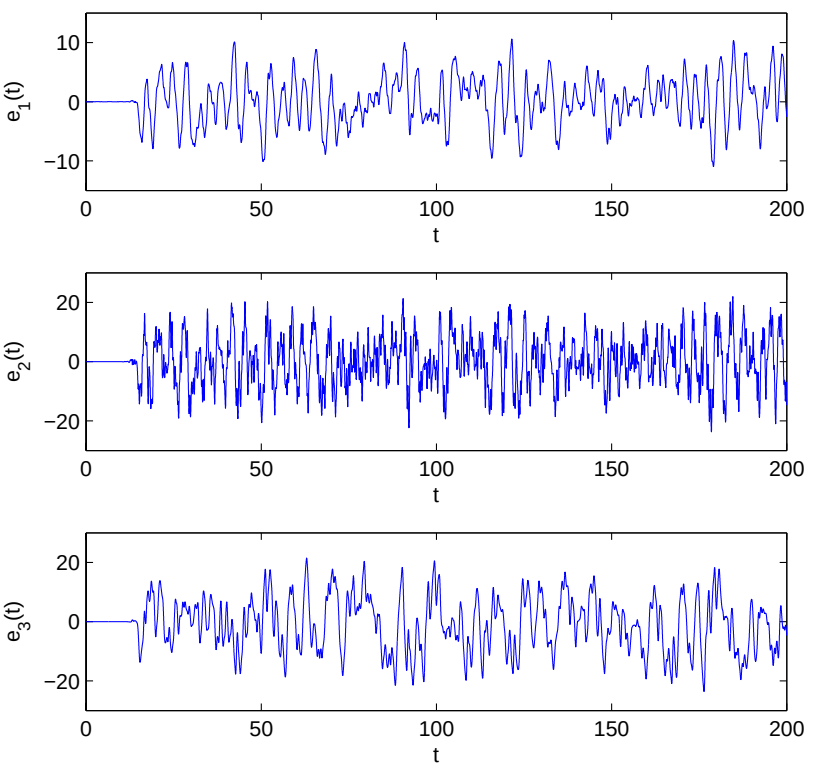

Fig. 2. The error evolution where $e_1(t) = x_1(t) - y_1(t)$, $e_2(t) = x_2(t) - y_2(t)$, and $e_3(t) = x_3(t) - y_3(t)$.

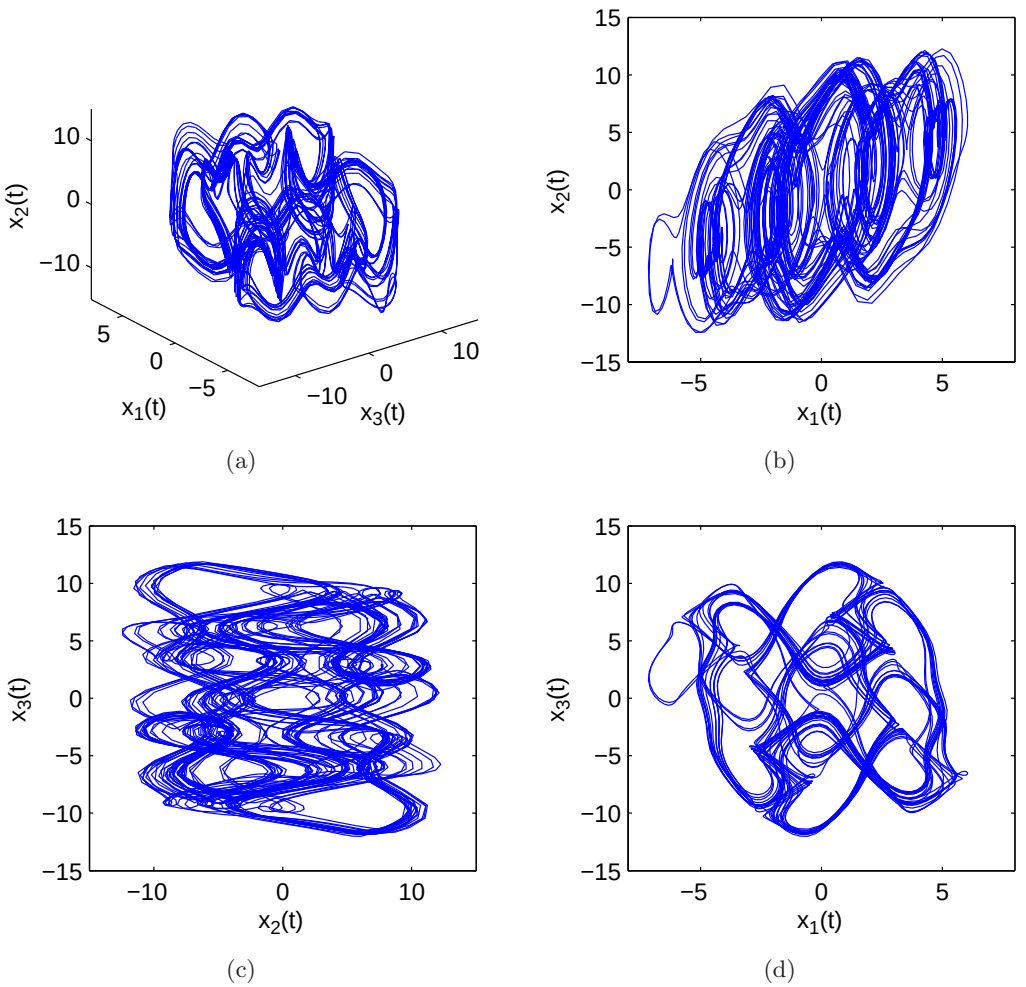

Fig. 3. (a) Chaotic attractor given by system (3) with $a_1 = -1$, $a_2 = 1$, $a_3 = -1$, $b_1 = 36$, and $b_2 = 18$. Projection of the chaotic attractor on the (b) x_1–x_2 plane, (c) x_2–x_3 plane and (d) x_1–x_3 plane.

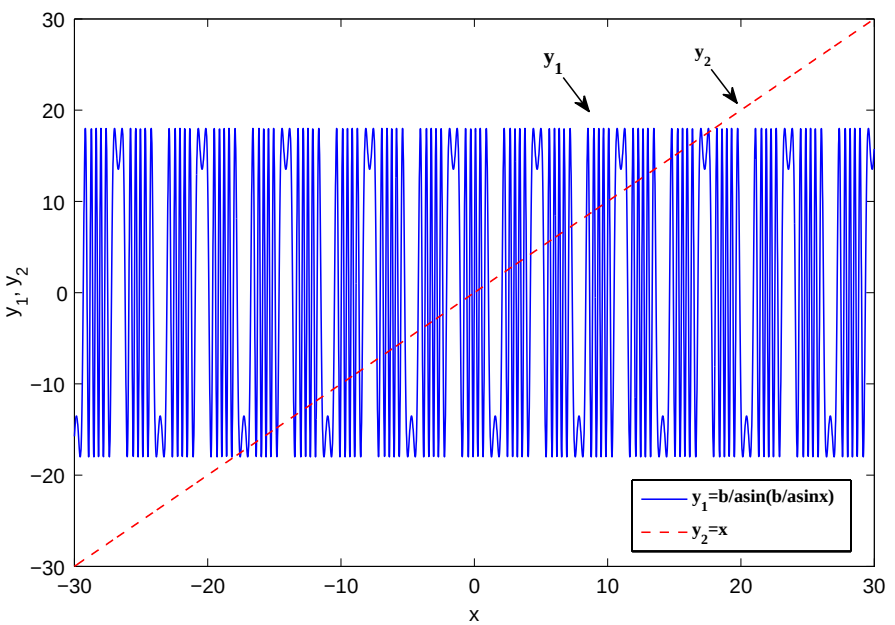

Fig. 4. The equilibrium points at which the intersections occur for $a = 1$ and $b = 5.3$.

Numerical computation shows that all equilibria are unstable. For instance, at $X^* = (0, 0, 0)$, its corresponding eigenvalues and eigenvectors are

$$\begin{aligned}\lambda_{1,2} &= -5.3075 \pm 7.5275i,\\ \lambda_3 &= 7.6150,\\ v_{1,2} &= w_1 \pm w_2 i\\ &= \begin{bmatrix} 0.0553\\ -0.9665\\ 0.1172\end{bmatrix} \pm \begin{bmatrix} 0.0967\\ 0\\ -0.1994\end{bmatrix} i,\\ v_3 &= \begin{bmatrix}0.1121\\ 0.9657\\ 0.2342\end{bmatrix}.\end{aligned}$$

Thus, the stable and unstable subspaces of Eq. (5) are $E^S = \text{Span}\{w_1, w_2\}$ and $E^U = \text{Span}\{v_3\}$, respectively. It implies that $X^* = (0, 0, 0)$ is an unstable saddle point.

2.2. *Dissipation and symmetry*

Dissipation: System (3) is dissipative.

Denote the unit volume of the flow of system (3) by V and we have

$$\begin{aligned}\nabla V &= \frac{\partial \dot{x}_1}{\partial x_1} + \frac{\partial \dot{x}_2}{\partial x_2} + \frac{\partial \dot{x}_3}{\partial x_3}\\ &= a_1 + a_1 + a_3 = -3a < 0.\end{aligned}$$

From the definition of dissipation, we say that system (3) is dissipative. It can be observed that a volume element V_0 at time t_0 will be contracted by the flow into $V_0 e^{-3a(t-t_0)}$ at time t, i.e. each volume containing the system trajectory shrinks to zero as $t \to \infty$ at an exponential rate $-3a$. Therefore, all trajectories of system (3) are ultimately confined to a specific subset with zero volume and its asymptotical behavior settles onto an attractor.

Symmetry: System (3) is symmetric with respect to the origin, which can be proved by the following transformation:

$$(x_1, x_2, x_3) \to (-x_1, -x_2, -x_3).$$

In terms of this symmetry, if $S^+(x_1^*, x_2^*, x_3^*)$ is an equilibrium point of system (3), then $S^-(-x_1^*, -x_2^*, -x_3^*)$ must be its equilibrium point. And if $\Gamma(x_1(t), x_2(t), x_3(t))$ $(t \geq t_0)$ is one of its trajectories, then $\Gamma(-x_1(t), -x_2(t), -x_3(t))$ also is its trajectory.

2.3. *Boundedness analysis*

In general, a system is said to be chaotic if it is bounded and possesses one positive Lyapunov exponent. In this subsection, we prove the boundedness of system (3).

Theorem 1. *System (3) is always bounded if* $a_1 < 0$ *and* $a_3 < 0$.

Proof. Define $V(t) = X(t)^T X(t)$. We have

$$\begin{aligned}V'(t) &= \dot{X}(t)^T X(t) + X(t)^T \dot{X}(t)\\ &= X(t)^T (A^T + A) X(t) + 2F^T B^T x(t)\\ &\leq 2\bar{a}\|X(t)\|^2 + 2\bar{b}\|F\|\|X(t)\|,\end{aligned}$$

where $\bar{a} = \max\{a_1, a_3\}$ and $\bar{b} = \max\{|b_1|, |b_2|\}$. Since

$$\|F\| = (\sin(x_1)^2 + \sin(x_3)^2)^{1/2} \leq \sqrt{2},$$

we have

$$V'(t) \leq 2\bar{a}\|X(t)\|^2 + 2\sqrt{2}\bar{b}\|X(t)\|.$$

Let $M = \frac{\sqrt{2}\bar{b}}{|\bar{a}|}$ and define

$$\begin{aligned}\Omega_0 &= \{X(t) \,|\, \|X(t)\| = M\}\\ \Omega_1 &= \{X(t) \,|\, \|X(t)\| \leq M\}.\end{aligned}$$

When $\|X(t)\| > M$, we obtain

$$V'(t) < 2M\bar{a}\|X(t)\| + 2\sqrt{2}\bar{b}\|X(t)\| = 0.$$

It implies that system (3) is bounded by Ω_0. All its trajectories outside Ω_1 will ultimately go into Ω_1 and will always be retained in Ω_1. ■

2.4. *Bifurcation and Lyapunov spectra*

It is well known that Lyapunov exponent (LE) characterizes the exponential rate of separation of infinitesimally close trajectories in phase space. A positive LE is usually taken as an indication of chaos, provided the dynamical system is bounded. We calculate the three LEs of system (3) as $\lambda_1 = 0.6032$, $\lambda_2 = -0.0019$ and $\lambda_3 = -3.6020$ for $a = 1$ and $b = 18$. The largest one is positive. Thus, combining with its boundedness, we say that system (3) is chaotic. And its Lyapunov dimension (Kaplan–Yorke dimension) can be calculated by

$$D_{KY} = k + \sum_{i=1}^{j} \frac{\lambda_i}{\lambda_{k+1}} = 2 + \frac{\lambda_1 + \lambda_2}{|\lambda_3|} = 2.1669,$$

where k is the maximum integer such that the sum of the k largest exponents is still non-negative. If $k = 0$, let $D_{KY} = 0$.

Next, we study the bifurcation diagram and Lyapunov spectra of system (3). Fix $a = 1$ and let b vary.

(1) For $b \in [0, 1)$, system (3) has a stable equilibrium point $(0, 0, 0)$;
(2) for $b = 1$, bifurcation occurs and $(0, 0, 0)$ loses stability and two new equilibria are generated, both of which are stable;
(3) for $b \in (1, 2.26)$, system (3) has three equilibria, one unstable equilibrium point $(0, 0, 0)$ and two new stable equilibria;
(4) for $b = 2.26$, bifurcation occurs and two stable equilibria lose stability and four new equilibria are generated, all of which are stable;
(5) for $b \in (2.26, 3.2494)$, system (3) has seven equilibria, three unstable equilibria and four new stable equilibria;
(6) for $b = 3.2494$, Hopf bifurcation occurs and four stable equilibria lose stability as a pair of complex conjugate eigenvalues of the linearization of system (3) around the equilibria cross the imaginary axis of the complex plane. All equilibria and corresponding eigenvalues are shown in Table 1;
(7) for $b \in (3.2494, 9.8]$, system (3) converges to a limit cycle;
(8) for $b > 9.8$, the chaotic behavior of system (3) appears.

Figure 5 shows the bifurcation diagram of x_1 versus b. The Lyapunov exponent spectra is shown in Fig. 6. The uppermost curve (the blue) denotes its maximal Lyapunov exponent, which is an indication of chaos. When this curve goes into the upper half plane, system (3) turns into chaos. It can be also observed that whenever the uppermost one becomes positive, the middle one (the green) rapidly approaches to zero. It is because of its continuity. At least one Lyapunov exponent vanishes (equal to 0) if the trajectory of an attractor does not contain a fixed point [Haken, 1983]. The Lyapunov dimension is shown in Fig. 7. From the definition of Lyapunov dimension, we know that for a three-dimensional autonomous system,

$$LD \begin{cases} \leq 2, & \text{for a nonchaotic system,} \\ > 2, & \text{for a chaotic system.} \end{cases}$$

Thus, the chaotic region of b (the shadow) can be clearly observed from Fig. 7.

Table 1. List of equilibrium points and the corresponding eigenvalues.

No.	Equilibrium Point	Eigenvalues
1	(0, 0, 0)	$\lambda_1 = 1.6435$
		$\lambda_{2,3} = -2.3218 \pm 2.4982i$
2–3	$(\pm 2.3383, \pm 2.3383, \pm 2.3383)$	$\lambda_1 = 1.0139$
		$\lambda_{2,3} = -2.0069 \pm 2.0104i$
4–7	$(\pm 1.0469, \pm 1.0469, \pm 2.8136)$	$\lambda_1 = -3.0000$
	$(\pm 2.8136, \pm 2.8136, \pm 1.0469)$	$\lambda_{2,3} = \pm 2.0001i$

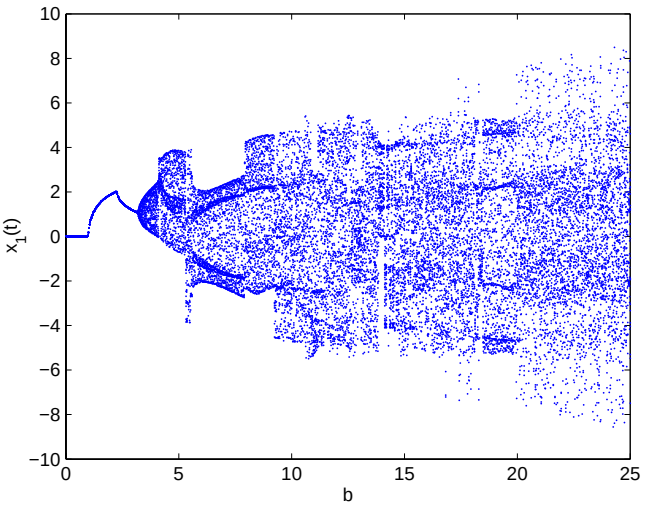

Fig. 5. The bifurcation diagram of $x_1(t)$ versus b, with $a = 1$.

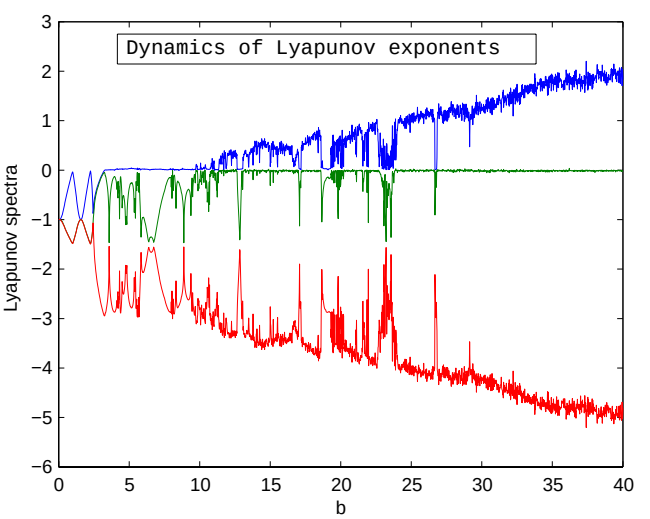

Fig. 6. The Lyapunov exponent spectra versus b, with $a = 1$.

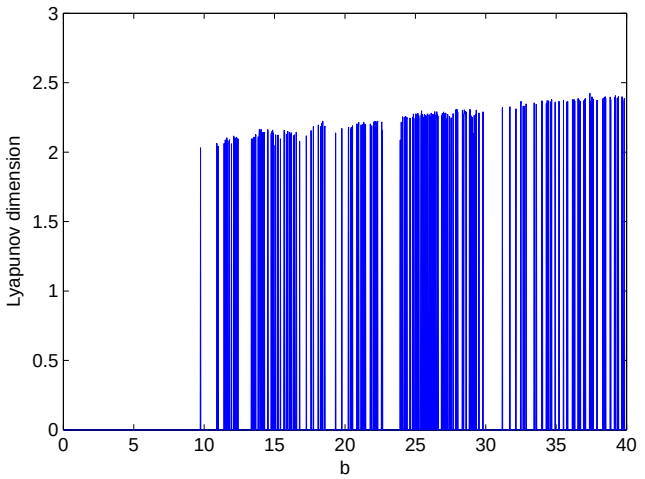

Fig. 7. The Lyapunov dimension versus b, with $a = 1$.

2.5. *The impact of the system parameter b*

It can be seen that the variation of b has a critical impact on the dynamical behavior of system (3) from the above bifurcation diagram and Lyapunov exponent spectra. With b increasing, the system alternately exhibits periodicity and chaos, starting from convergence to a fixed point. Here, we further explore various chaotic attractors and periodic orbits in detail with b varying.

For $b = 12$, system (3) has a simpler attractor, as shown in Fig. 8. Its three LEs are: $\lambda_1 = 0.3068$, $\lambda_2 = -0.0013$ and $\lambda_2 = -3.3057$. The largest one is positive, which implies that system (3) is chaotic.

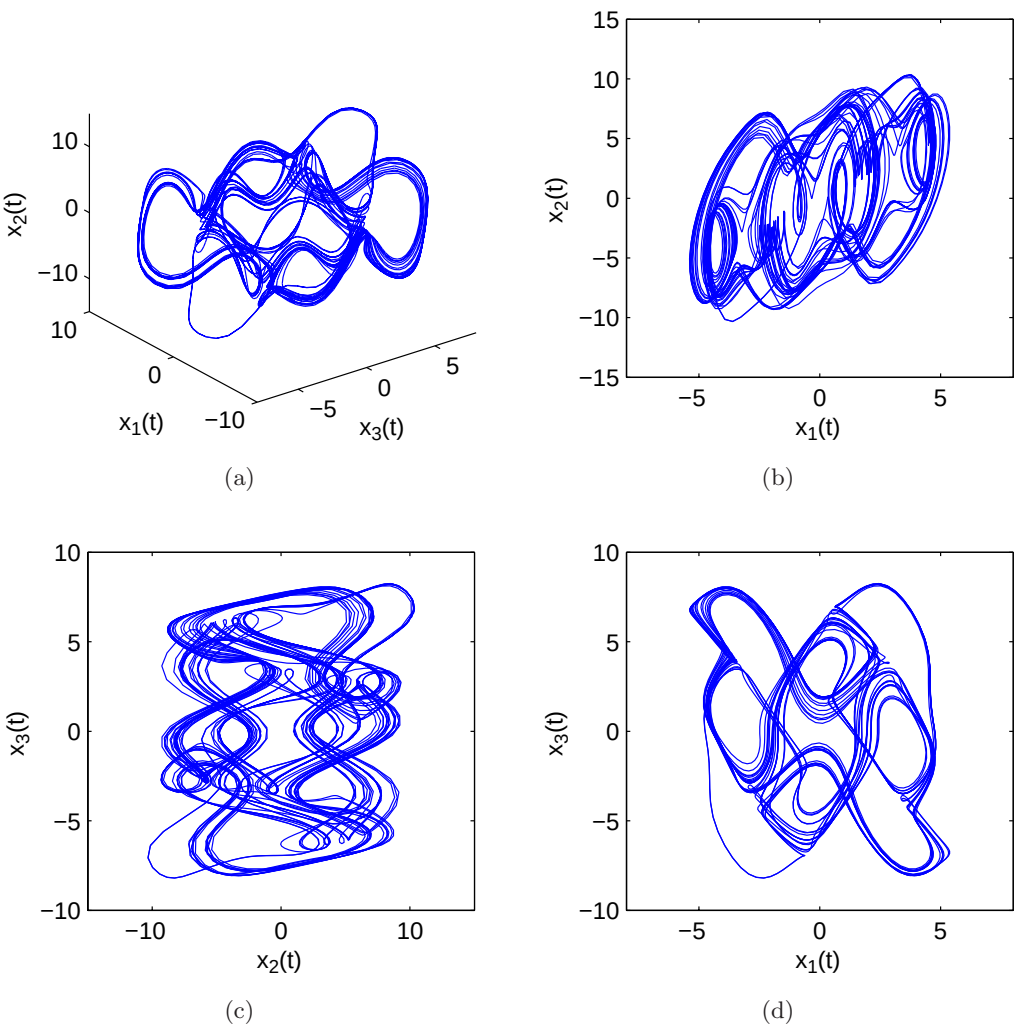

Fig. 8. (a) New chaotic attractor given by system (3) with $a_1 = -1$, $a_2 = 1$, $a_3 = -1$, $b_1 = 24$, and $b_2 = 12$. Projection of the chaotic attractor on the (b) x_1–x_2 plane, (c) x_2–x_3 plane and (d) x_1–x_3 plane.

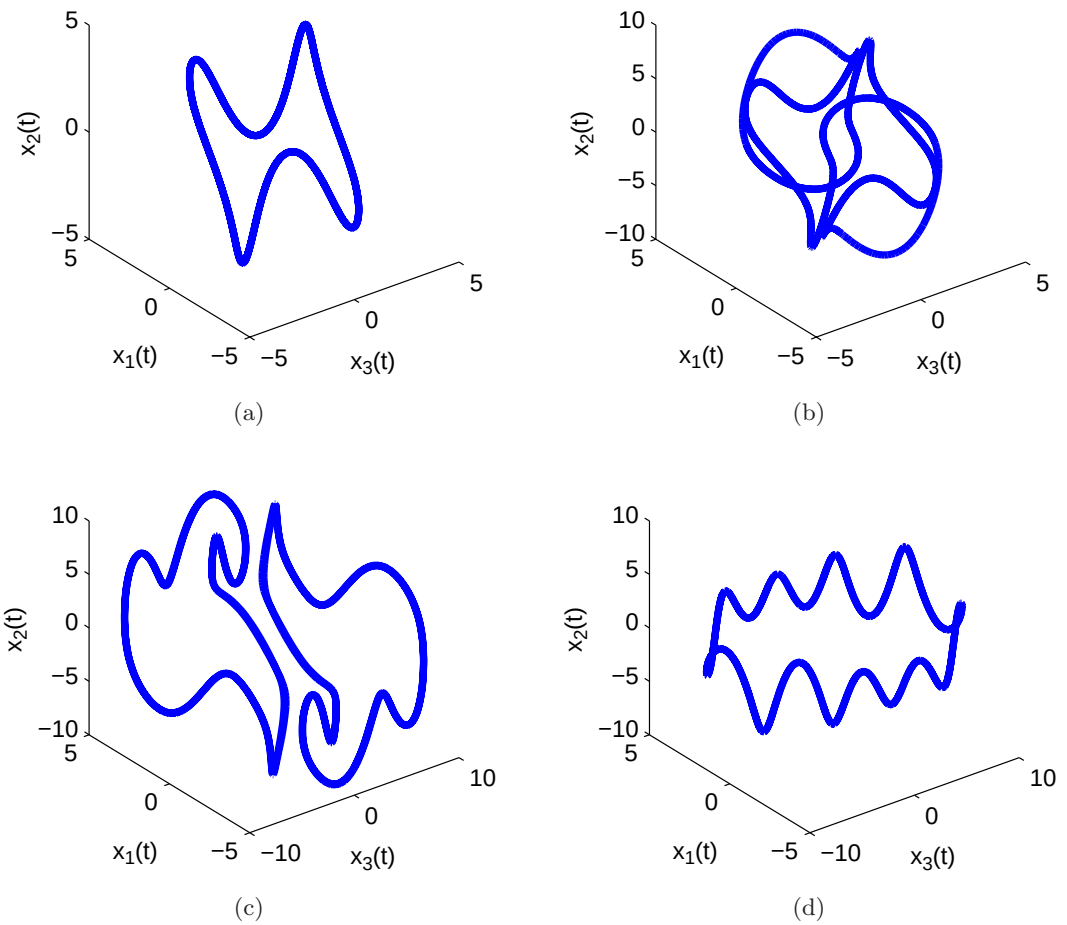

Fig. 9. Periodic orbits, (a) $b = 6$, (b) $b = 8$, (c) $b = 14$ and (d) $b = 23$.

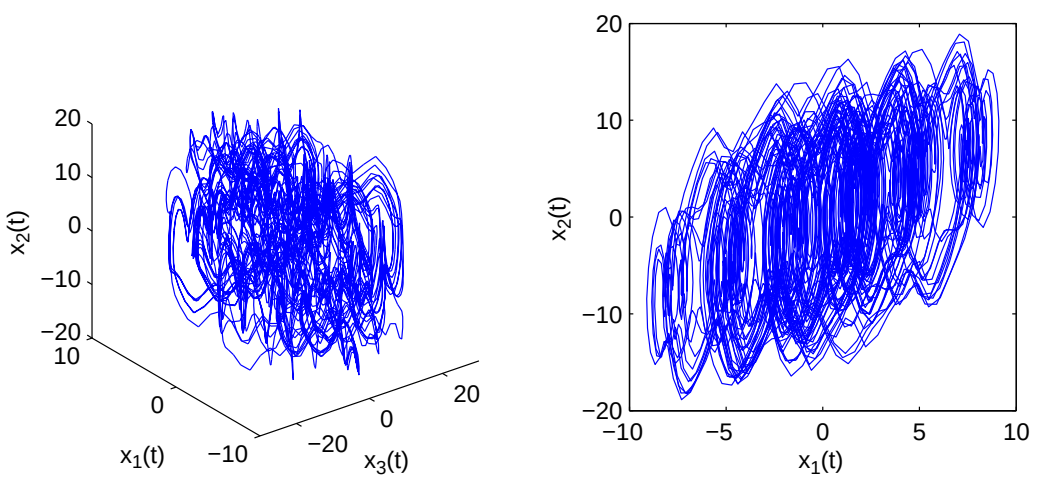

Fig. 10. (a) New chaotic attractor given by system (3) with $a_1 = -1$, $a_2 = 1$, $a_3 = -1$, $b_1 = 68$, and $b_2 = 34$. Projection of the chaotic attractor on the (b) x_1–x_2 plane, (c) x_2–x_3 plane and (d) x_1–x_3 plane.

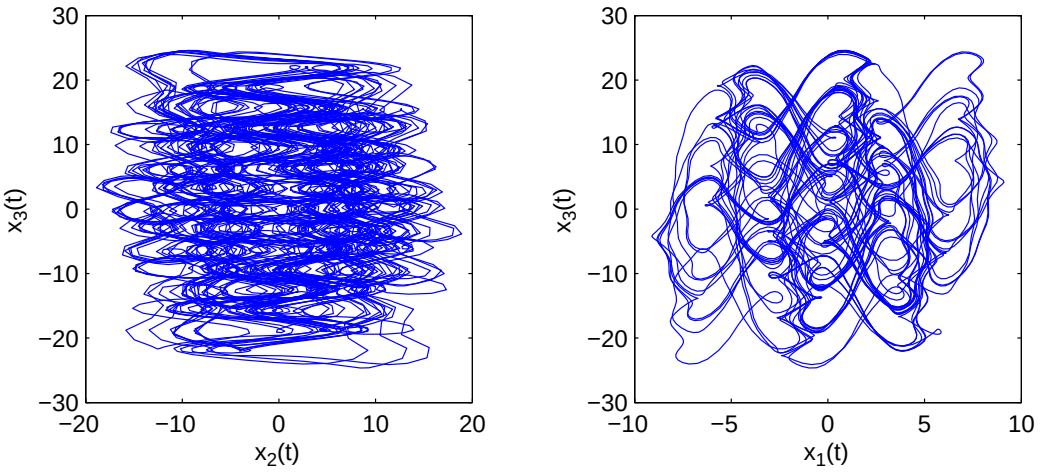

(c) (d)

Fig. 10. (*Continued*)

For $b = 6, 8, 14, 23$, system (3) exhibits various periodic orbits, as shown in Fig. 9. Chaotic and periodic dynamics appear alternately with b increasing.

For $b = 34$, system (3) has a more complex chaotic attractor, as shown in Fig. 10. Its three LEs are: $\lambda_1 = 1.7125$, $\lambda_2 = -0.0008$ and $\lambda_2 = -4.7127$.

Remark 1. It is well known that the maximal LE of an attractor dominates the exponential stretching and folding of its orbits, i.e. the value of the largest positive LE measures the degree of the disorder of the attractor. With b further increasing ($b > 24$), the maximal LE of system (3) is positive almost everywhere and also keeps increasing, which causes more complex dynamical behavior.

3. Chaos Entanglement

Chaos phenomenon was first discovered by Henri Poincaré, who found that there exist some orbits that are nonperiodic, and yet not forever increasing nor approaching a fixed point when studying the three-body problem, in the 1880s. However, it seems that chaos only exists in rare and specific circumstances, not like stable systems, periodic systems, diverging system that exist far and wide in reality. Up to now, almost all chaotic attractors are found casually and disappear with slight change of some system parameters. Does there exist a systematical method to generate chaos? Chaos entanglement is proposed to solve this problem. Our chaos entanglement scheme consists of two parts: a set of linear subsystems and entanglement functions. Two conditions should be satisfied to generate chaos:

(1) all linear subsystems are stable and approach a fixed point;
(2) all entanglement functions are periodic and bounded.

Condition (1) guarantees that the system has a folding strength to pull back its trajectories when they are going too far. Condition (2) guarantees that the system has a stretching strength to push away its trajectories when they are approaching too close to the equilibrium points.

3.1. *Chaos entanglement with different subsystems*

It is well known that autonomous continuous systems have at least three dimensions to generate chaos. Therefore, we choose one two-dimensional and one one-dimensional subsystems in system (3). In fact, the number of subsystems is not limited to two and the subsystems are not necessary to be identical in system parameters and even in dimension. Labyrinth chaos [Thomas, 1999; Sprott & Chlouverakis, 2007] is a good example, including three identical linear subsystems entangled by sine function. Here, we entangle three linear subsystems with different parameters and different dimensions. One is two-dimensional and two are one-dimensional:

Three subsystems are given by,

$$\dot{X}_i = -A_i X_i,$$

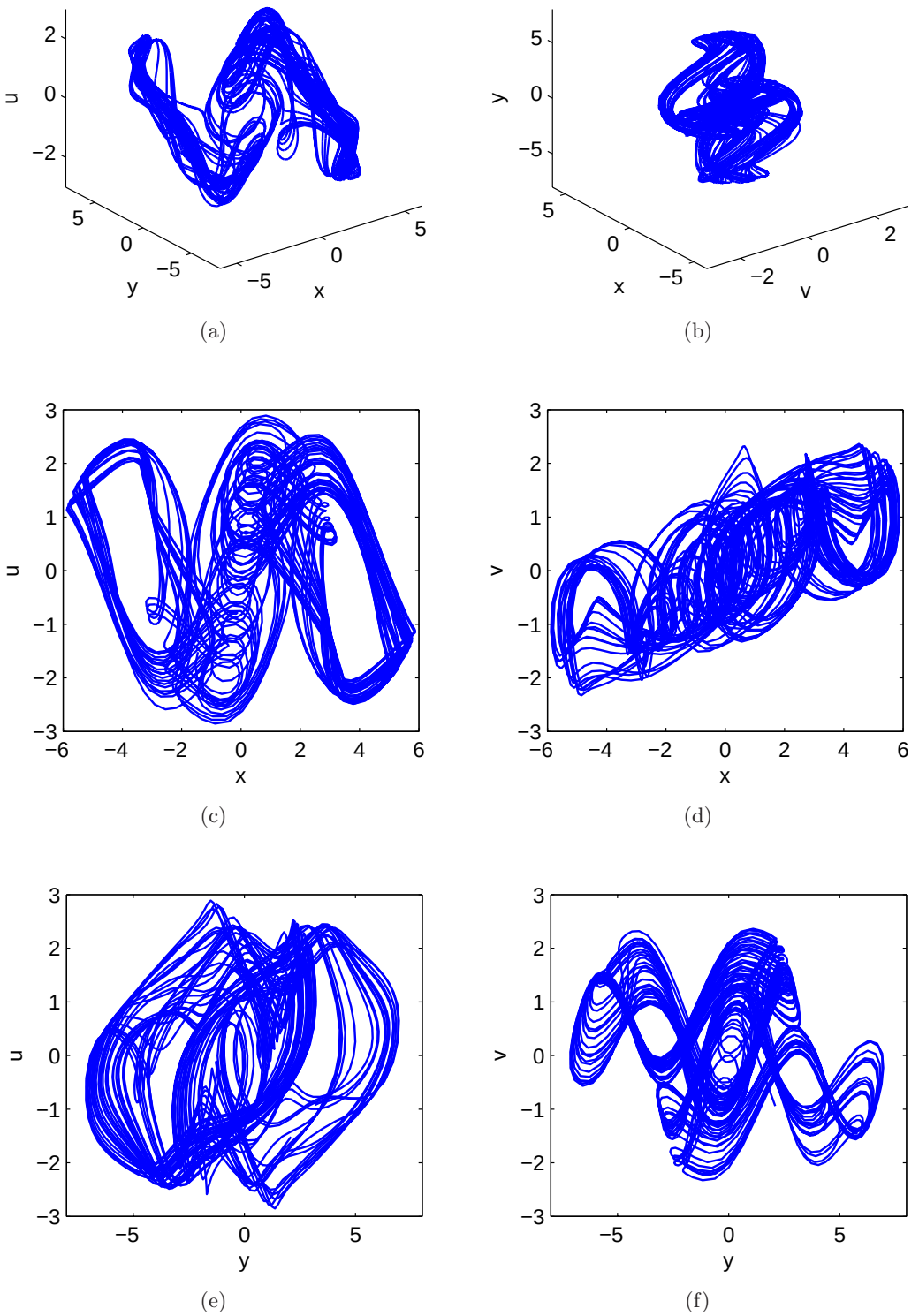

Fig. 11. Projection of a four-dimensional chaotic attractor entangled by one two-dimensional and two one-dimensional subsystems with $a = 1$ and $b = 8.2$ on the (a) $x - y - u$ space, (b) $v - x - y$ space, (c) x–u plane, (d) x–v plane, (e) y–u plane and (f) y–v plane.

where $i = 1, 2, 3$, $X_1 = [x, y]^T$, $X_2 = u$, $X_3 = v$, and

$$A_1 = \begin{bmatrix} a_1 & a_1 \\ -a_1 & a_1 \end{bmatrix}, \quad A_2 = a_2, \quad A_3 = a_3.$$

The entanglement coefficients and functions are:

$$B = \begin{bmatrix} b & 0 & 0 & 0 \\ 0 & b & 0 & 0 \\ 0 & 0 & b & 0 \\ 0 & 0 & 0 & b \end{bmatrix}, \quad F = \begin{bmatrix} \sin(v) \\ \sin(u) \\ \sin(x) \\ \sin(y) \end{bmatrix}.$$

When $a_1 = 1$, $a_2 = 2$, $a_3 = 3$, and $b = 8.2$, chaos entanglement is achieved. The three-dimensional and two-dimensional phase portraits, $x - y - u$, $v - x - y$, x–u, x–v, y–u, and y–v, are shown in Fig. 11. Numerical computation shows this system has four Lyapunov exponents as $\lambda_1 = 0.7655$, $\lambda_2 = 0.0003$, $\lambda_3 = -3.2538$, and $\lambda_4 = -4.5109$.

Remark 2. In terms of different subsystems entangled, the chaotic attractors generated are totally different, with different structures, different dimensions, different number of equilibria, etc. Along this way, a lot of strange attractors can be generated.

3.2. *Chaos entanglement with different entanglement functions*

It is very clear that entanglement function plays a critical role in chaos entanglement. Its periodicity and boundedness are required according to

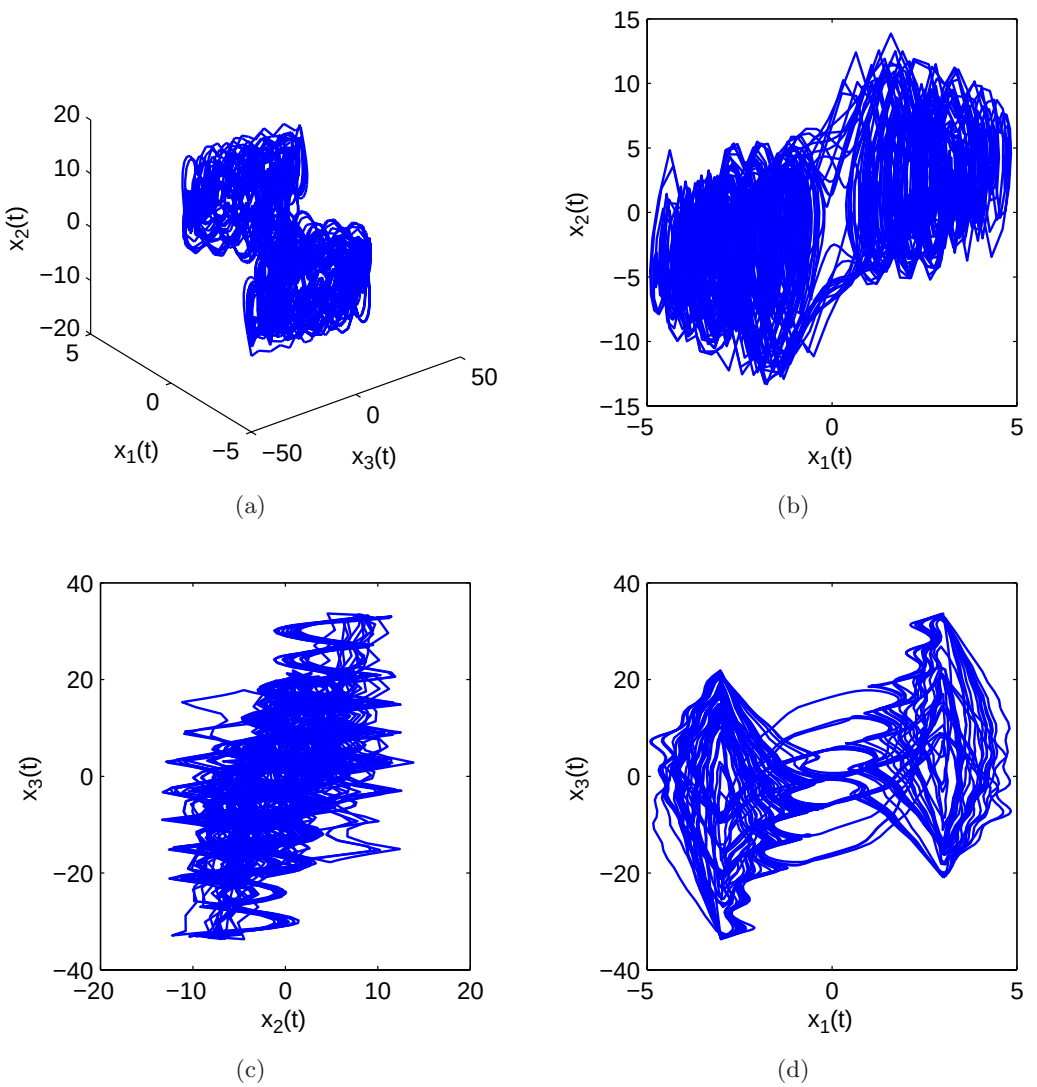

Fig. 12. (a) New chaotic attractor entangled by piecewise linear entanglement function with $a = 1$ and $b = 18$. Projection of the chaotic attractor on the (b) x_1–x_2 plane, (c) x_2–x_3 plane and (d) x_1–x_3 plane.

condition (2). In this subsection, we consider different entanglement functions to generate chaos.

(1) Chaos entanglement with piecewise linear function

Consider the same subsystems, (1) and (2). Replace $\sin(\cdot)$ by the following piecewise linear function $g(\cdot)$, described by

$$g(x) = \begin{cases} x - k\omega, & k\omega \le x < \left(k + \frac{1}{2}\right)\omega; \\ x - (k+1)\omega, & \left(k + \frac{1}{2}\right)\omega \le x < (k+1)\omega; \end{cases}$$

where $k = 0, \pm 1, \pm 2, \ldots$ and the period length is $\omega = 6$.

Similarly, the entanglement coefficients and entanglement functions are:

$$B = \begin{bmatrix} 0 & 0 & 0 \\ 0 & b_1 & 0 \\ 0 & 0 & b_2 \end{bmatrix} \quad \text{and} \quad F = \begin{bmatrix} 0 \\ g(x_3) \\ g(x_1) \end{bmatrix}.$$

When $a = 1$ and $b = 18$, i.e. $a_1 = -1$, $a_2 = 1$, $a_3 = -1$, $b_1 = 36$ and $b_2 = 18$, chaos entanglement is realized. The phase portraits, $x_1(t)-x_2(t)-x_3(t)$, $x_1(t)$–$x_2(t)$, $x_2(t)$–$x_3(t)$, and $x_3(t)$–$x_1(t)$ are shown in Fig. 12.

Remark 3. Chaos entanglement with piecewise linear function can be thought of as a switching linear system, but it is definitely new, different from the one in [Campos-Cantón *et al.*, 2010]. For instance,

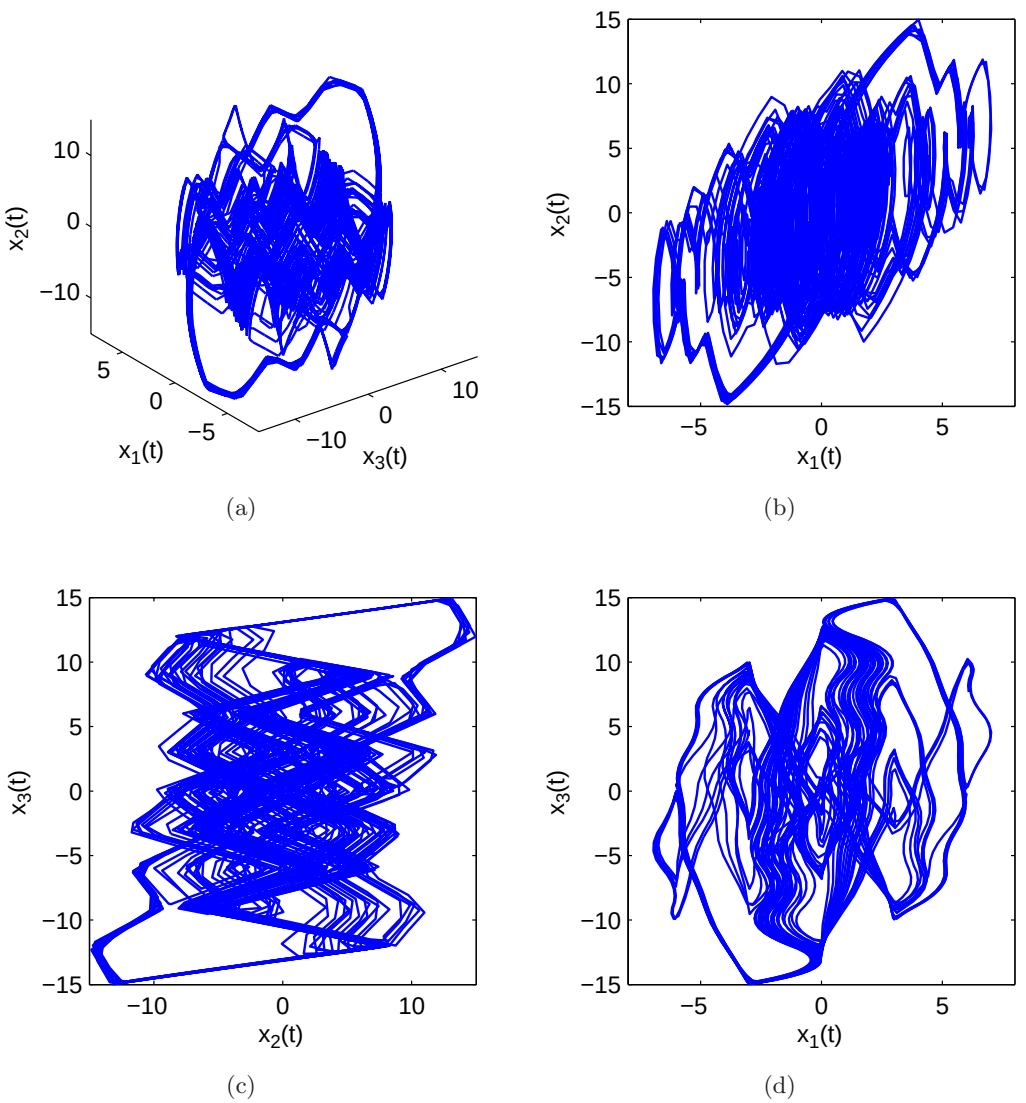

Fig. 13. (a) New chaotic attractor entangled by piecewise sign entanglement function with $a = 1$ and $b = 18$. Projection of the chaotic attractor on the (b) x_1–x_2 plane, (c) x_2–x_3 plane and (d) x_1–x_3 plane.

the conditions $\tau = \mathrm{Tr}(A) < 0$, $\gamma = a_{11}a_{22} + a_{11}a_{22} + a_{22}a_{33} - a_{13}a_{31} - a_{23}a_{32} - a_{12}a_{21} > 0$, and $\delta = \det(A) < 0$ are required in [Campos-Cantón *et al.*, 2010]. While in our system, $A = \begin{pmatrix} -1 & 1 & 0 \\ -1 & -1 & 36 \\ 18 & 0 & -1 \end{pmatrix}$, $\delta = \det(A) = 646 > 0$ does not satisfy the above conditions. Also, the difference between them can be observed from the eigenvalues. In our system, three eigenvalues are followed, $\lambda_1 = 7.6150$, $\lambda_{2,3} = -5.3075 \pm 7.5275i$, which are not in the desired form of the above reference, one negative real root and two complex conjugates with positive real part.

(2) Chaos entanglement with piecewise sign function

The subsystems and entanglement coefficients are the same as above. Consider the following piecewise sign function $g(x)$, given by,

$$g(x) = \begin{cases} 1, & k\omega \le x < \left(k + \dfrac{1}{2}\right)\omega; \\ -1, & \left(k + \dfrac{1}{2}\right)\omega \le x < (k+1)\omega; \end{cases}$$

where $k = 0, \pm 1, \pm 2, \ldots$ and the period length is $\omega = 6$.

When $a = 1$ and $b = 18$, chaos entanglement is realized. The phase portraits, $x_3(t) - x_1(t) - x_2(t)$, $x_1(t)$–$x_2(t)$, $x_2(t)$–$x_3(t)$, and $x_1(t)$–$x_3(t)$ are shown in Fig. 13.

4. Circuit Implementation

In this section, a possible electronic circuit is given to realize system (3), as shown in Fig. 14. This circuit includes three layers, each of which implements one equation of system (3). For instance, layer 1 (dash-dot rectangle 1) is used to realize

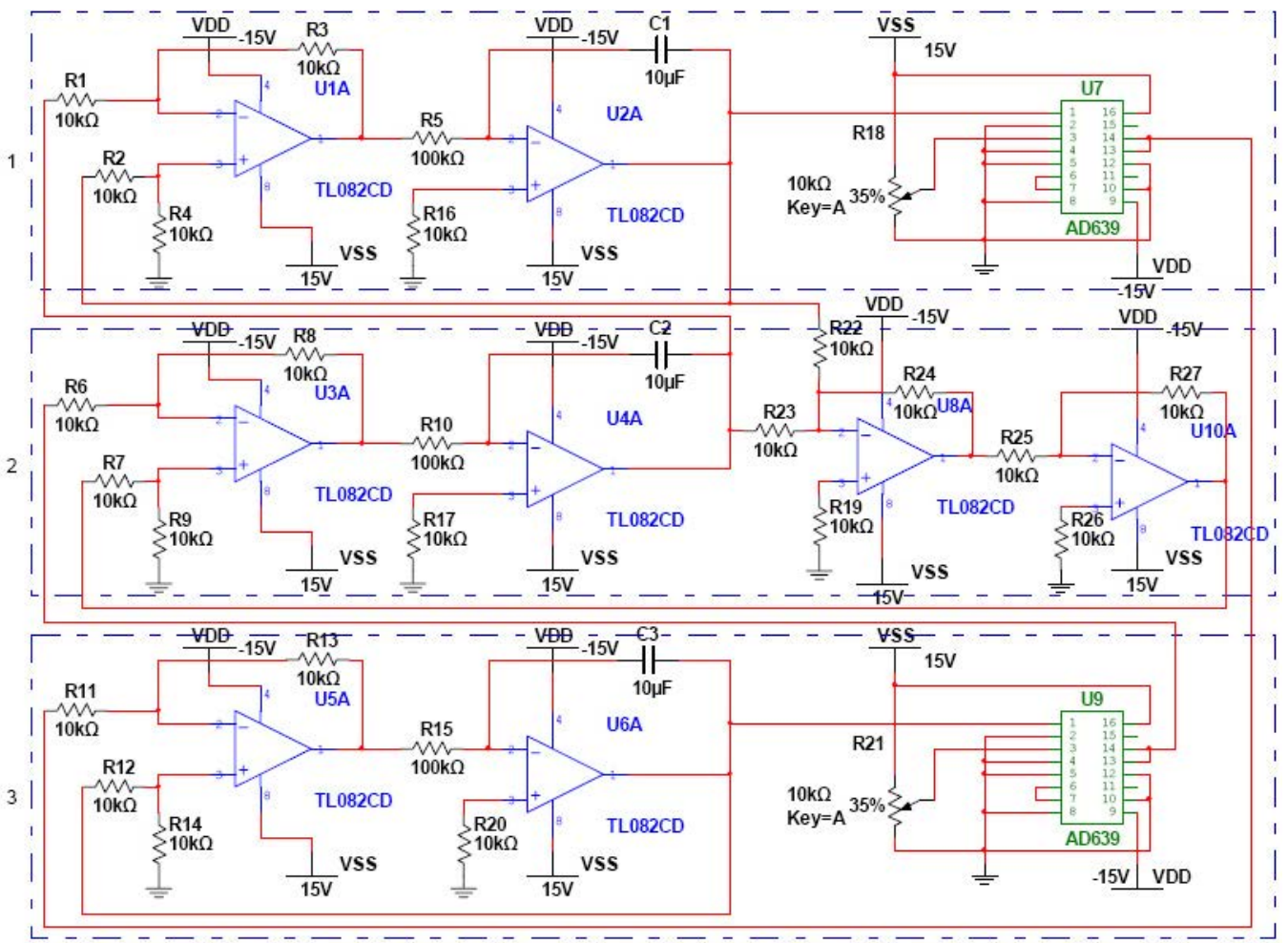

Fig. 14. Electronic circuit diagram for generating the new attractor system (3).

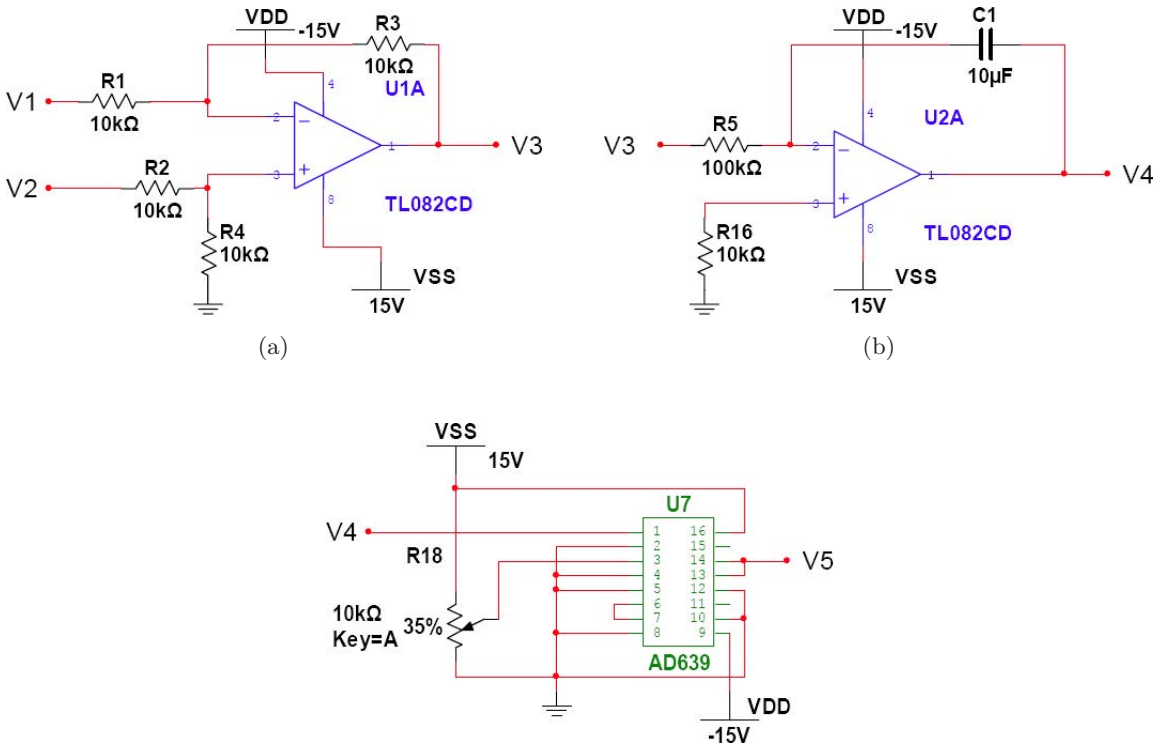

Fig. 15. Circuit blocks: (a) prepositive subtracting circuit, (b) integrating circuit and (c) sine function circuit.

$\dot{x}_1 = -x_1 + x_2$. The output of U2A is x_1. Similarly, x_2 and x_3 are denoted by the outputs of U4A and U6A, respectively.

Layer 1 consists of three parts: a prepositive subtracting circuit, an integrating circuit and a sine function circuit. The prepositive subtracting circuit [shown in Fig. 15(a)] can be described by

$$\frac{V_1 - \dfrac{R_4}{R_2 + R_4}V_2}{R_1} + \frac{V_3 - \dfrac{R_4}{R_2 + R_4}V_2}{R_3} = 0.$$

When $R_1 = R_3$ and $R_2 = R_4$, we have

$$V_3 = V_2 - V_1.$$

The integrating circuit [Fig. 15(b)] can be described by

$$C_1\frac{dV_4}{dt} + \frac{V_3}{R_5} = 0.$$

When $R_5C_1 = 1$, we have

$$\frac{dV_4}{dt} = -V_3.$$

The sine function circuit employs a commercial trigonometric function chip AD639 (U7). The detailed set-up is shown in Fig. 15(c). The system parameter b_1 can be adjusted by the variable resistor $R18$, i.e.

$$\begin{cases} V_5 = b_1 \sin(V_4), \\ b_1 = 80\% \times 15 = 12. \end{cases}$$

Thus,

$$\frac{dV_4}{dt} = -V_3 = -(V_2 - V_1) = -V_4 + V_1.$$

Select the output voltages of the integrating circuits as state variables x_i, $i = 1, 2, 3$. We obtain

$$\begin{cases} \dot{x}_1 = -x_1 + x_2 \\ \dot{x}_2 = -x_1 - x_2 + b_1 \sin(x_3) \\ \dot{x}_3 = -x_3 + b_2 \sin(x_1). \end{cases}$$

5. Conclusion

We have proposed a new approach to generate artificial chaos by entangling two or multiple stable linear subsystems. Dynamical analysis and numerical simulation have demonstrated that the new attractor is dissipative, symmetric with respect to the origin, and possesses a positive Lyapunov exponent. Furthermore, we have generated a variety of novel

chaotic attractors by choosing different subsystems and different entanglement functions. Our discovery solves the requirement for new chaotic systems in engineering applications, which can be utilized as a guideline for constructing new chaotic attractors. To further improve this method, there are two outstanding issues needed to be addressed. One is if it is possible to entangle a set of periodic or diverging linear subsystems to generate chaos, while the other is how to generate hyper-chaos by chaos entanglement. In future work, we will furthermore explore various possible connections between linear systems and chaos, establish the sufficient conditions for chaos entanglement to generate chaos, and try to find out the essence of chaos.

Acknowledgments

The authors would like to thank the reviewers and the associate editor for their valuable comments and suggestions which improved the quality of the paper.

References

Ahmad, W. & Sprott, J. [2003] "Chaos in fractional-order autonomous nonlinear systems," *Chaos Solit. Fract.* **16**, 339–351.

Campos-Cantón, E., Barajas-Ramírez, J., Solís-Perales, G. & Femat, R. [2010] "Multiscroll attractors by switching systems," *Chaos* **20**, 013116.

Čelikovský, S. & Chen, G. [2002] "On a generalized Lorenz canonical form of chaotic systems," *Int. J. Bifurcation and Chaos* **12**, 1789–1812.

Chen, G. & Ueta, T. [1999] "Yet another chaotic attractor," *Int. J. Bifurcation and Chaos* **9**, 1465–1466.

Chua, L., Wu, C., Huang, A. & Zhong, G. [1993] "A universal circuit for studying and generating chaos. I. Routes to chaos," *IEEE Trans. Circuits Syst.-I*: *Fund. Th. Appl.* **40**, 732–744.

Elwakil, A. & Kennedy, M. [2001] "Construction of classes of circuit-independent chaotic oscillators using passive-only nonlinear devices," *IEEE Trans. Circuits Syst.-I*: *Fund. Th. Appl.* **48**, 289–307.

Elwakil, A. & Ozoguz, S. [2006] "Multiscroll chaotic oscillators: The nonautonomous approach," *IEEE Trans. Circuits Syst.-II*: *Exp. Briefs* **53**, 862–866.

Haken, H. [1983] "At least one Lyapunov exponent vanishes if the trajectory of an attractor does not contain a fixed point," *Phys. Lett. A* **94**, 71–72.

Hartley, T., Lorenzo, C. & Killory Qammer, H. [1995] "Chaos in a fractional order Chua's system," *IEEE Trans. Circuits Syst.-I*: *Fund. Th. Appl.* **42**, 485–490.

Li, C. & Chen, G. [2004] "Chaos in the fractional order Chen system and its control," *Chaos Solit. Fract.* **22**, 549–554.

Li, Y., Liu, X. & Zhang, H. [2005] "Dynamical analysis and impulsive control of a new hyperchaotic system," *Math. Comput. Model.* **42**, 1359–1374.

Liu, X., Teo, K., Zhang, H. & Chen, G. [2006] "Switching control of linear systems for generating chaos," *Chaos Solit. Fract.* **30**, 725–733.

Liu, X., Shen, X. & Zhang, H. [2012] "Multi-scroll chaotic and hyperchaotic attractors generated from Chen system," *Int. J. Bifurcation and Chaos* **22**, 1250033.

Lorenz, E. [1963] "Deterministic nonperiodic flow," *J. Atmosph. Sci.* **20**, 130–141.

Lu, H. & He, Z. [1996] "Chaotic behavior in first-order autonomous continuous-time systems with delay," *IEEE Trans. Circuits Syst.-I*: *Fund. Th. Appl.* **43**, 700–702.

Lü, J. & Chen, G. [2002] "A new chaotic attractor coined," *Int. J. Bifurcation and Chaos* **12**, 659–661.

Lü, J., Chen, G., Yu, X. & Leung, H. [2004a] "Design and analysis of multiscroll chaotic attractors from saturated function series," *IEEE Trans. Circuits Syst.-I*: *Reg. Papers* **51**, 2476–2490.

Lü, J., Han, F., Yu, X. & Chen, G. [2004b] "Generating 3-d multi-scroll chaotic attractors: A hysteresis series switching method," *Automatica* **40**, 1677–1687.

Lü, J. & Chen, G. [2006] "Generating multiscroll chaotic attractors: Theories, methods and applications," *Int. J. Bifurcation and Chaos* **16**, 775.

Mackey, M. & Glass, L. [1977] "Oscillation and chaos in physiological control systems," *Science* **197**, 287–289.

Matsumoto, T. [1984] "A chaotic attractor from Chua's Circuit," *IEEE Trans. Circuits Syst.* **31**, 1055–1058.

Namajunas, A., Pyragas, K. & Tamasevicius, A. [1995] "An electronic analog of the Mackey–Glass system," *Phys. Lett. A* **201**, 42–46.

Pecora, L. & Carroll, T. [1990] "Synchronization in chaotic systems," *Phys. Rev. Lett.* **64**, 821–824.

Sprott, J. [2007] "A simple chaotic delay differential equation," *Phys. Lett. A* **366**, 397–402.

Sprott, J. & Chlouverakis, K. [2007] "Labyrinth chaos," *Int. J. Bifurcation and Chaos* **17**, 2097–2108.

Suykens, J. & Vandewalle, J. [1993] "Generation of n-double scrolls ($n = 1, 2, 3, 4, \ldots,$)," *IEEE Trans. Circuits Syst.-I*: *Fund. Th. Appl.* **40**, 861–867.

Tamasevicius, A., Mykolaitis, G. & Bumeliene, S. [2006] "Delayed feedback chaotic oscillator with improved spectral characteristics," *Electron. Lett.* **42**, 736–737.

Tang, W., Zhong, G., Chen, G. & Man, K. [2001] "Generation of n-scroll attractors via sine function," *IEEE Trans. Circuits Syst.-I*: *Fund. Th. Appl.* **48**, 1369–1372.

Thomas, R. [1999] "Deterministic chaos seen in terms of feedback circuits: Analysis, synthesis, 'labyrinth chaos'," *Int. J. Bifurcation and Chaos* **9**, 1889–1906.

Vaněček, A. & Čelikovský, S. [1996] *Control Systems*: *From Linear Analysis to Synthesis of Chaos* (Prentice Hall International (UK) Ltd.).

Wang, L. & Yang, X. [2006] "Generation of multi-scroll delayed chaotic oscillator," *Electron. Lett.* **42**, 1439–1441.

Watts, R. [2007] *Global Warming and the Future of the Earth* (Morgan & Claypool).

Yalçin, M., Suykens, J., Vandewalle, J. & Ozoguz, S. [2002] "Families of scroll grid attractors," *Int. J. Bifurcation and Chaos* **12**, 23–42.

Yalçin, M. [2007] "Multi-scroll and hypercube attractors from a general jerk circuit using Josephson junctions," *Chaos Solit. Fract.* **34**, 1659–1666.

Yalçin, M. & Özoguz, S. [2007] "n-scroll chaotic attractors from a first-order time-delay differential equation," *Chaos* **17**, 033112.

Yu, S., Lu, J. & Chen, G. [2007] "Multifolded torus chaotic attractors: Design and implementation," *Chaos* **17**, 013118.

Zhang, H., Liu, X., Shen, X. & Liu, J. [2012] "A family of novel chaotic and hyperchaotic attractors from delay differential equation," *Dyn. Contin., Discr. Impul. Syst. Series B*: *Appl. Algorith.* **19**, 411–430.